Carbon fixation of CO_2 via cyclic reactions with borane in gaseous atmosphere leading to formic acid (and metaboric acid); A potential energy surface (PES) study

Marziyeh Mohammadi[1]*, Seyyed Amir Siadati[2]*,
Sheida Ahmadi[3], Sepideh Habibzadeh[3],
Mohammad Reza Poor Heravi[3], Zinatossadat Hossaini[2] and
Esmail Vessally[3]

[1]Department of Chemistry, Faculty of Science, Vali-e-Asr University of Rafsanjan, Rafsanjan, Iran,
[2]Department of Chemistry, Qaemshahr Branch, Islamic Azad University, Qaemshahr, Iran,
[3]Department of Chemistry, Payame Noor University, Tehran, Iran

Carbon dioxide (CO_2), a stable gaseous species, occupies the troposphere layer of the atmosphere. Following it, the environment gets warmer, and the ecosystem changes as a consequence of disrupting the natural order of our life. Due to this, in the present reasearch, the possibility of carbon fixation of CO_2 by using borane was investigated. To conduct this, each of the probable reaction channels between borane and CO_2 was investigated to find the fate of this species. The results indicate that among all the channels, the least energetic path for the reaction is reactant complex (RC) to TS (A-1) to Int (A-1) to TS (A-D) to formic acid (and further meta boric acid production from the transformation of boric acid). It shows that use of gaseous borane might lead to controlling these dangerous greenhouse gases which are threatening the present form of life on Earth, our beautiful, fragile home.

KEYWORDS

carbon dioxide, atmospheric pollution, borane cycle, reaction channels, CO_2 fixation, metaboric acid

Introduction

Carbon dioxide has been one of the most dangerous threats to the present order of our lives. As one of the major greenhouse gases, it makes our environment warmer and directly changes the ecosystem of Earth, the only known planet in the cosmos that supports complex life forms (Herndon and Whiteside, 2021).

On the one hand, in spite of the global attempts of scientists, the amount of CO_2 released into the atmosphere is increasing annually (Abrantes et al., 2021). On the other

GRAPHICAL ABSTRACT
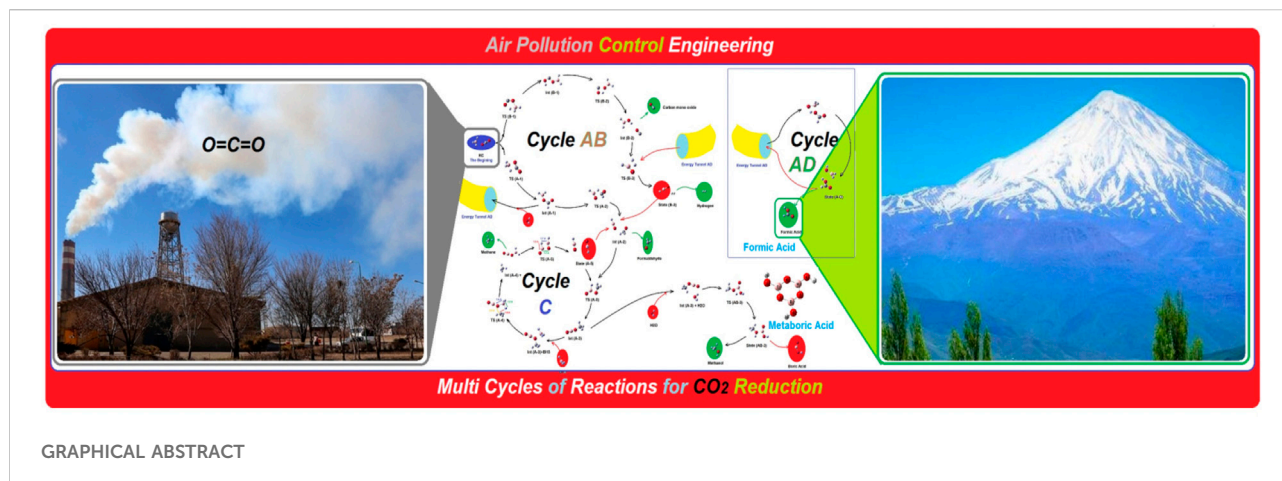
hand, replacing fossil fuels with green energy resources could not be carried out in the near future. Thus, stopping of CO_2 emissions into the atmosphere could not be an operational approach, at least in the present decade (York and Bell, 2019). Instead, researchers have found different ways to store or use such polluting species (Yang et al., 2021; Liu et al., 2022; Pandey et al., 2022). Artificial photosynthesis (Keijer et al., 2021), electrochemical reduction (Lin et al., 2019; Zhao and Quan, 2021), and also chemical reactions (Pramudita and Motokura, 2021; Porgar and Rahmanian, 2022) are some of those approaches.

At least at the present time, it seems that chemical reactions might be one of the most practical approaches for reduction of CO_2 (Sharghi et al., 2017; Santos-Carballal et al., 2021). The chemical reactions could be run in the absence of electrical energy or fragile systems, which are required for artificial photosynthesis.

Previous reports reveal that some of the borane derivatives (in the presence of catalysts) could be a choice for chemical reduction of CO_2 due to their ability to release negative hydrogen atoms. As an example, in recent years, Kadota et al. (2019) have successfully used metallic borohydrides in the presence of triphenylphosphine as the catalyst and acetonitrile as the solvent to give a porous coordination polymer (Kadota et al., 2019). In another work (2020), they used calcium borohydrides in the presence of pyridine derivatives as the catalyst and dimethylsulfoxide (DMSO) as a solvent at 40°C to consume CO_2 for the production of calcium formate (Kadota et al., 2020). In addition, Zhu et al. (2019), reacted lithium and sodium borohydrides to CO_2 in a gas–solid phase system for 24 h to yield hydrogen molecule and trimethylborane (Zhu et al., 2019). Also, there are some other examples in which metallic borohydrides, mostly in the presence of the base and solvent, have reacted to CO_2 to yield synthesized composites or other products (Fujiwara et al., 2014; Bontemps, 2016). In addition, sensing or attracting CO_2 by special nano-structures via chemical

reactions was studied and proved to be performable in some previous reports. It indicates that some of the electron-rich components are able to reduce this gaseous species (Siadati et al., 2016a; Pakravan and Siadati, 2017; Vessally et al., 2017; Kadhim et al., 2022a; Kadhim et al., 2022b; Li and Zhao, 2022). Also, the findings of the previous reports show that studying the mechanism of the reactions by using the PES method and reaction pathways approach could give valuable information about the fate of the atomic and molecular interactions between the chemical species (Siadati, 2015; Siadati et al., 2016b; Mohtat et al., 2018; Kula et al., 2021; Vessally and Hosseinian, 2021).

Due to the abovementioned issues, in this work, we attempted to follow each of the possible reaction subways between CO_2 and borane in order to find the fate of this system. The results of the PES studies and also the molecular dynamic simulations showed that formic acid (and further metaboric acid production from transformation of boric acid) would form finally from the reaction between CO_2 and borane, at least in the gas phase.

Calculation details

After performing the molecular dynamic simulations for the atomic system (containing boron, carbon, 3*hydrogen, and 2*oxygen), a number of meta-stable species (which might emerge via different atomic orientations) were detected. Then, after design and optimization of each separated molecule (BH_3, and CO_2), any interaction that could occur (despite energy peaks and any other barrier) was considered and input into the software to give any possible reaction pathway. After extracting the results via optimization of each atomic state, various reaction pathways with separated or common meta-stable species were designed. Those species consisted of reactant complexes, transition states (TSs), intermediates, and final products. The Gaussian

FIGURE 1
Results of the trajectory diagram for the molecular dynamic simulation based on energy per time (in femtosecond) (fs).
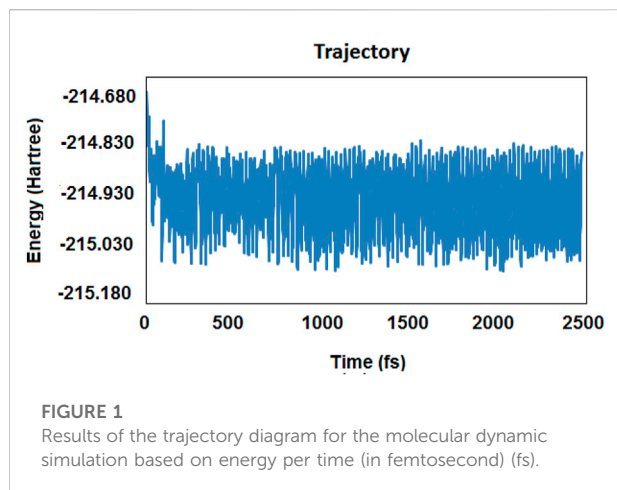
03 chemical quantum package (Frisch et al., 2003) was applied to perform the calculations, and the density functional theory (DFT) procedure at the B3LYP/6-311++G (d,p) level of theory was used to optimize the possible structures (Becke, 1988; Lee et al., 1988). The TS structures were recognized by using the synchronous transit-guided quasi-Newton (STQN) approach (Peng et al., 1996). In addition, in order to find the electrical charge of each atom in the reactants, intermediates, products, and TSs, the natural bond orbital (NBO) analysis was used (Reed et al., 1988).

The following formula was applied for calculating the global electron density transfer (GEDT):

$$GEDT = \sum q_A. \tag{1}$$

In which q_A is the net atom in molecule (AIM) charge (calculated by AIMAll (Version 10.07.01) (Keith, 2010; Domingo et al., 2021)) and the sum covered the entire atoms of CO_2 species.

Also, molecular dynamic simulations were performed to investigate the behavior of the mentioned atoms (Lawan et al., 2022).

Results and discussion

To investigate the possibility of CO_2 reduction by the gaseous form of borane (which evaporates at about 65°C to 67°C), all possible interactions between those two species were designed in order to make an accurate map. There were several reaction pathways with different orientations, intermediates, and products as the final state of energy. Moreover, a number of species came from different routes, which could form the cycles. The results of the molecular dynamic simulations helped us recognize some of the species that might emerge during the reaction coordinate (Figure 1). The simulation part of the

calculations was performed by using Gaussian 03 software. The classical trajectory calculation using the Born–Oppenheimer molecular dynamics model (BOMD) was performed in about 2473 femtoseconds (fs) (as the total simulation time). The force field was calculated with the aid of the DFT method; the temperature was set at 400 K, and the time-step was about 0.618 fs.

As shown in Figure 2 (Scheme 1), there were two primitive routes which produced a number of different reaction valleys (as sub-branches). Each of those sub-branches reaching a product or was linked to a cycle.

As shown in Figure 2, there are three main cycles which are linked to each other, by pillars of energy. Those are cycles AB, AD, and cycle C, which produce carbon monoxide, molecular hydrogen, and formaldehyde (cycle AB); methane and methanol (cycle C); and formic acid (cycle AD), respectively. At the beginning, there were no compounds except CO_2, and BH_3, while after the production of two primitive routes (containing routes A and B), and the formation of cycle AB, several meta-stable species with a variety of energy barriers, peaks, and valleys have emerged. Each of those would be described in the following sub-sections.

Cycle AB, reaction channels, and products

As shown in Figures 2, 3, at the first step, the primary reactant complex (containing CO_2, and BH_3) approaches each other in different orientations, which causes two separated main routes to emerge (channels A and B as well as the formation of cycle AB). Channel A is produced when 1 C=O bond of CO_2 comes closer to one B–H bond of borane (a side-by-side position) to produce **TS (A-1),** with an energy barrier of 15.11 kcal mol $^{-1}$ (making this process possible in view of energy). Also, channel B emerges *via* formation of a five-membered ring (**TS (B-1)**) during proton transfer from the boron atom of BH_3 to the free oxygen of CO_2. The energy barrier of this species is about 67.99 kcal mol $^{-1}$, which shows that route B needs a lot of thermal energy; somehow, in usual temperatures and in ambient systems, hypothetical channel A is formed much faster than its parallel route (channel B). Despite the fact that channel B is nearly banned at the energy barrier of **TS (B-1)**, it is mentioned that the subsequent stages of that route contain **Int (B-1)** (23.29 kcal mol $^{-1}$), **TS (B-2)** (51.38 kcal mol $^{-1}$; barrier = 28.09 kcal mol $^{-1}$), **Int (B-2)** (-18.11 kcal mol $^{-1}$), **TS (B-3)** (59.56 kcal mol $^{-1}$; barrier = 77.67 kcal mol $^{-1}$), and **state (B-3)** [releasing a molecular hydrogen and a HBO species into cycle C *via* **Int (A-2)**]. Thus, channel B is forbidden from the kinetic point of view. **Int (B-2)** releases a carbon monoxide molecule before the formation of **TS (B-3)**. Also, the results of the calculations show that in **TS (A-1)**, the amount of GEDT is about −0.242 (indicating the global electron transfer from CO_2 to borane, while the amount of this parameter for **Int (A-1)** is

FIGURE 2
Complex of the main routes and sub-branched reaction valleys for the reduction process of CO_2 by borane in gas phase.
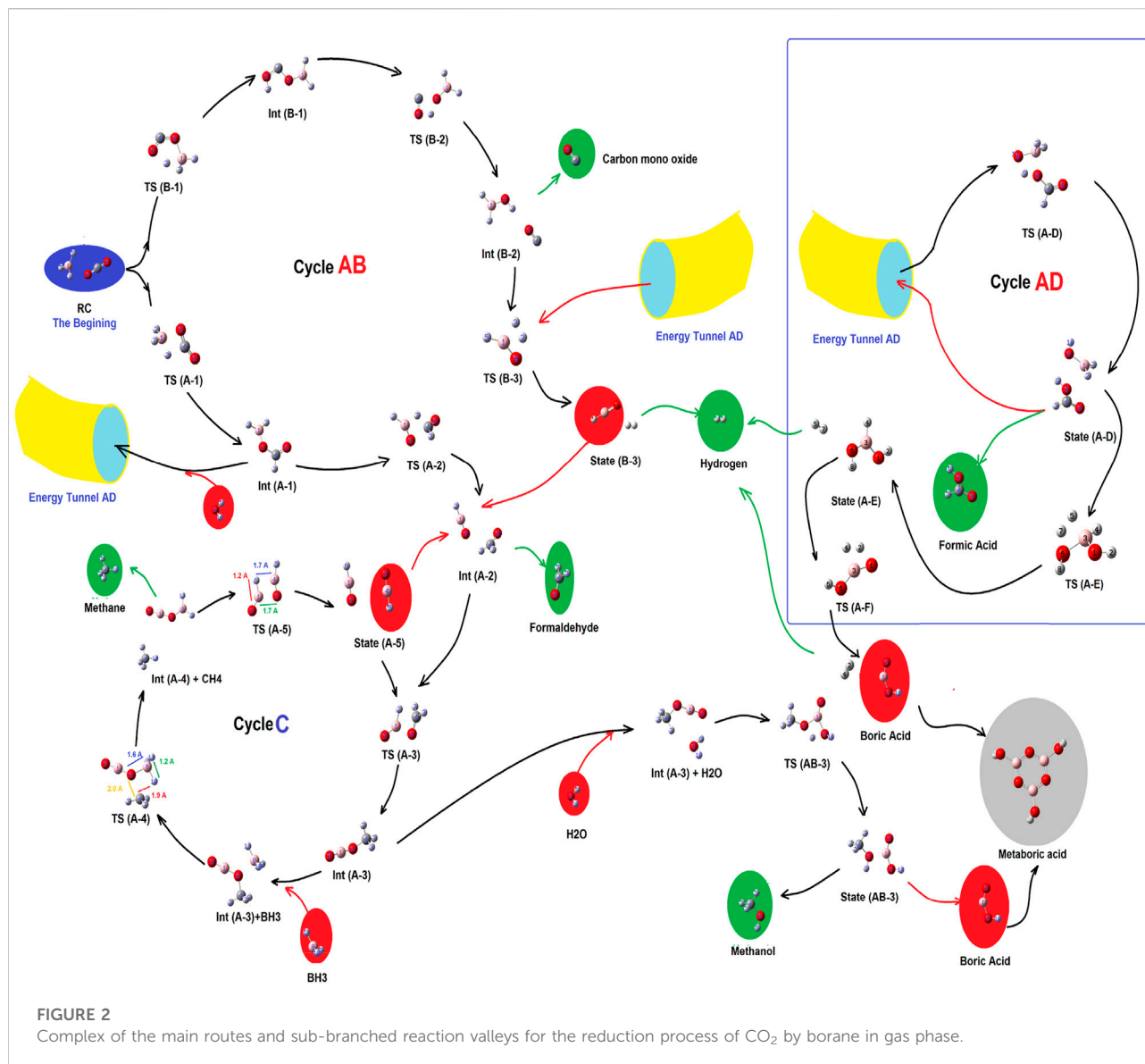
about −0.847 (attacking the electron density from borane segment to CO_2).

In channel A, **TS (A-1)** (15.11 kcal mol^{-1}) transforms to **Int (A-1)** (−19.73 kcal mol^{-1}), **TS (A-2)** (24.41 kcal mol^{-1}; barrier = 44.14 kcal mol^{-1}), and **Int (A-2)** (−14.22 kcal mol^{-1}), which completes cycle AB. Also, it seems that reaching **Int (A-2)** *via* channel A is difficult, but this route is still favored compared to channel B. Subsequently, **Int (A-2)** could release formaldehyde or transform **TS (A-3)** to form cycle C. It must be noted that at the middle of channel A, **Int (A-1)** could react with a single water molecule and pass through the reaction pathway AD and form **TS (A-D)**, having a relative energy barrier of 14.70 kcal mol^{-1}. Thus, moving **Int (A-1)** and H_2O to the reaction pathway A–D could give valuable information about the fate of the reaction cycles of the CO_2–borane complex.

Cycle C, reaction channels, and products

Cycle C would begin with the transformation of **Int (A-2)** into **TS (A-3)**. In this case, the formaldehyde part of **Int (A-2)** moves to reach a parallel situation with HBO species; somehow, the H–B bond of HBO approaches the O=C bond of formaldehyde. Then, the proton of HBO is transferred to the carbon of formaldehyde to yield **Int (A-3),** which is extremely stable even in comparison with RC (-54.33 kcal mol^{-1}). For the next step of this cycle, another BH_3 species attacks **Int (A-3)** and forms an **Int (A-3)-BH3** system. Then, it receives energy and turns into **TS (A-4)** with an energy content of 47.31 kcal mol^{-1} compared to the **Int (A-3)-BH$_3$** system (which could only proceed in high temperatures or some irradiative environments). In addition, this TS loses energy and reaches
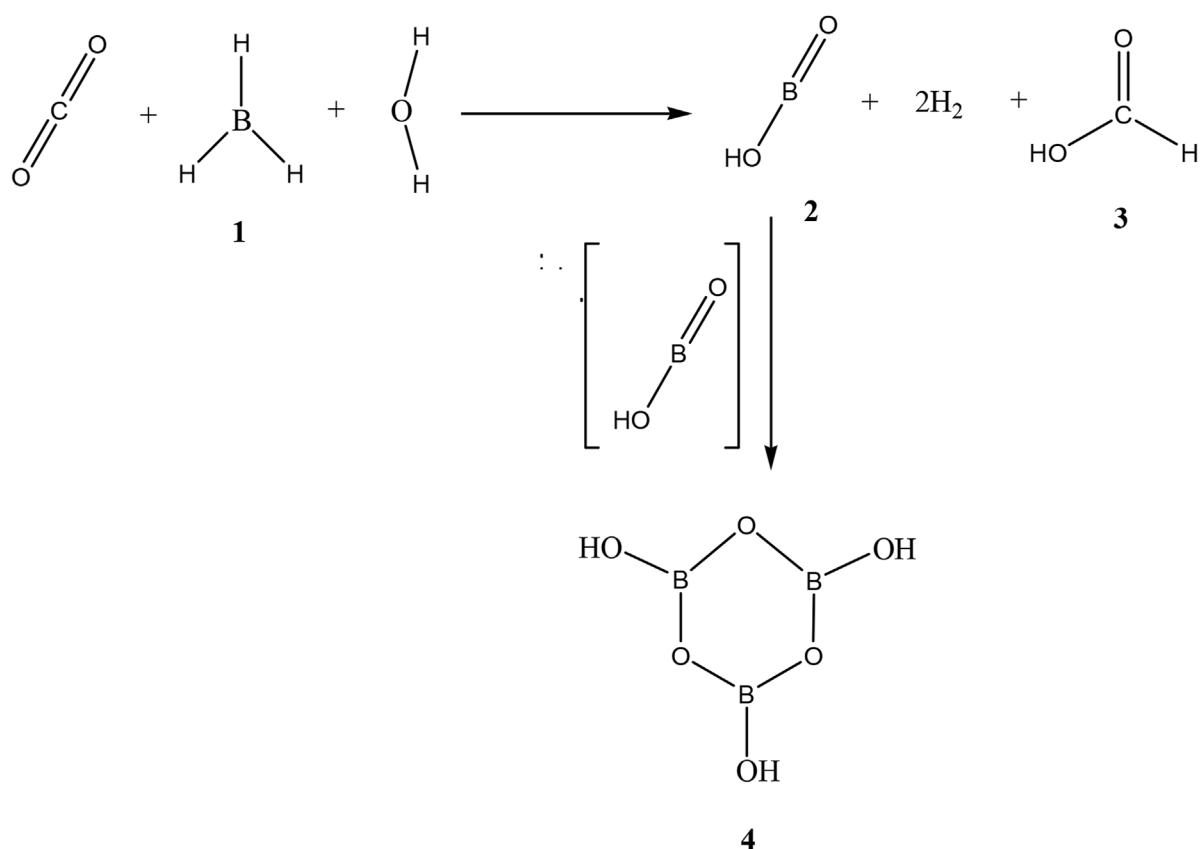
SCHEME 1
Total scheme of the reaction between CO_2 and borane **1,** leading to production of formic acid **3**, mono boric acid **2**, and metaboric acid trimer **4**.
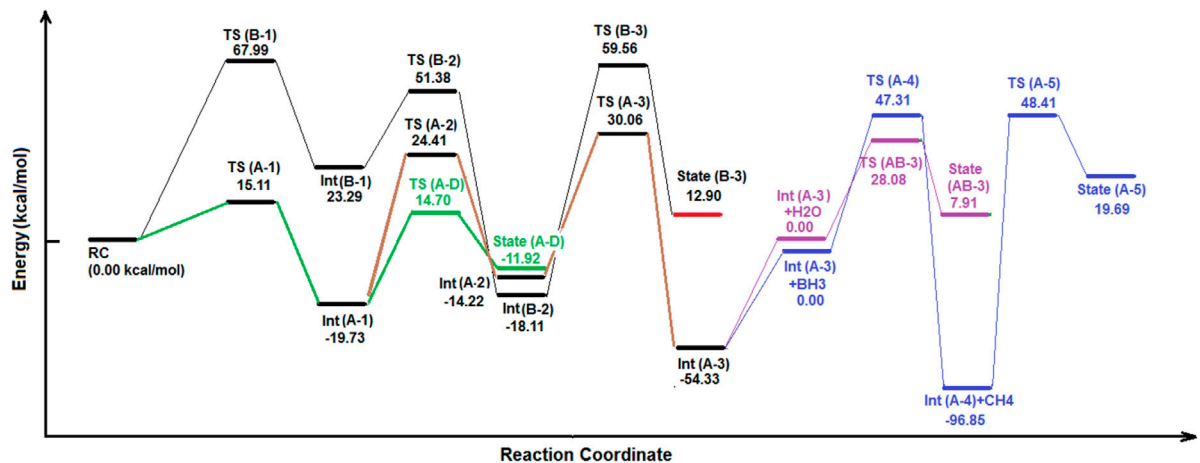
FIGURE 3
Energy diagram based on the reaction progress at B3LYP/6-311++G (d,p) level of theory.

FIGURE 4
Geometrical structures of all detected species which emerge during the reaction coordinate optimized at B3LYP/6-311++G (d,p) level of theory.
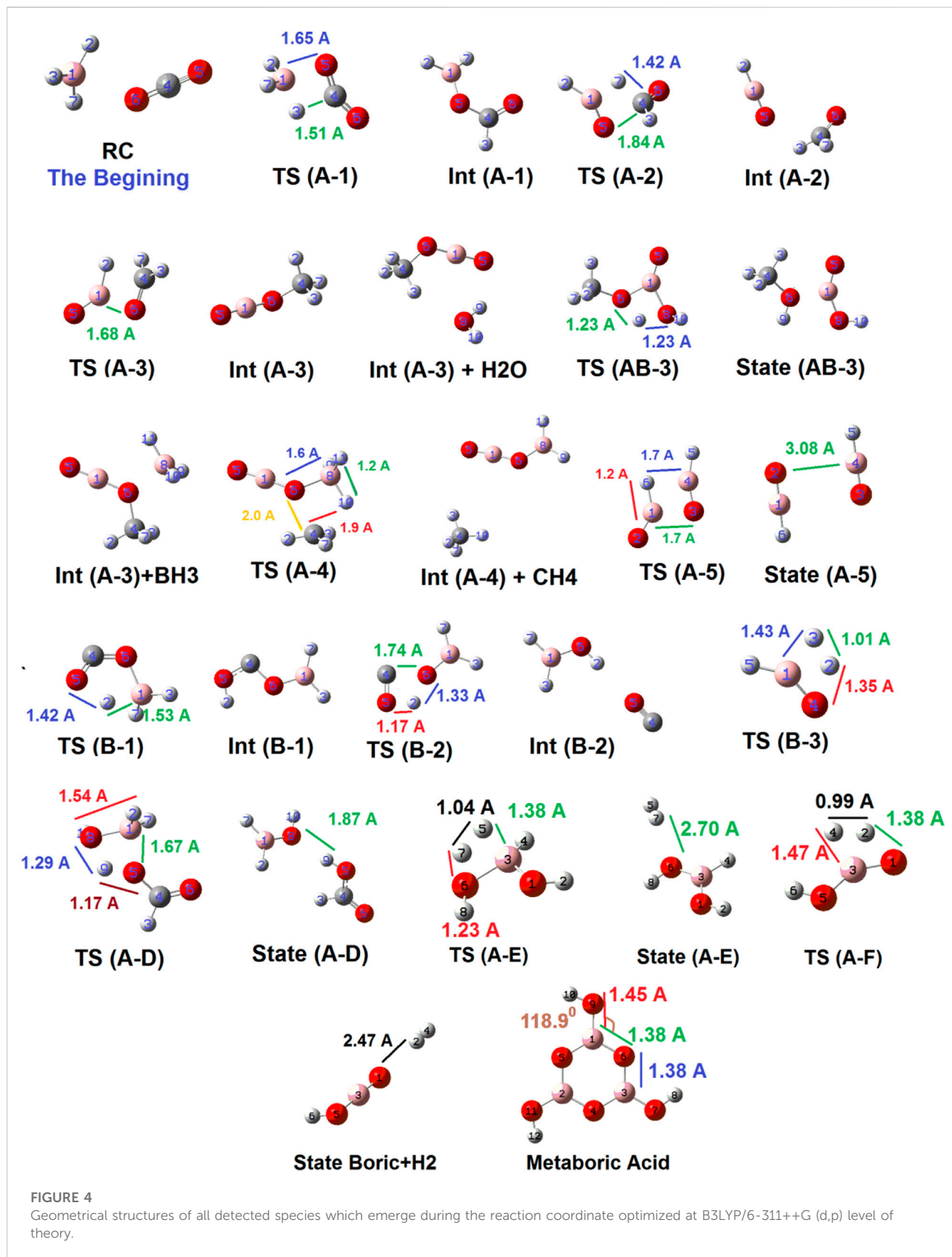
TABLE 1 Thermodynamic parameters as well as the negative frequency values of TSs for the possible reaction route.

TS	$\Delta G^{\#}$ (kcal mol^{-1})	$\Delta H^{\#}$ (kcal mol^{-1})	$\Delta S^{\#}$ (cal mol^{-1} K^{-1})	Negative freq (cm^{-1})
TS (A-1)	14.79	19.54	−15.93	−457.90
TS (A-D)	17.57	18.94	−4.57	−1262.52

the **Int (A-4) + CH$_4$** system with a relative PES of -96.85 kcal mol^{-1} (the lowest energy of whole cycles). It shows that in spite of high activation energies, which makes it kinetically unfavorable (at least in ambient conditions), the formation of some products of these cycles is extremely favored in view of thermodynamics. Then, the **Int (A-4)+CH$_4$** complex releases a methane molecule, and Int (A-4) (H$_2$BOBO) decomposes into two equal HBO fragments (**state (A-5)**), with an energy content of 19.69 kcal mol^{-1} compared to Int (A-4)) *via* the **TS (A-5)** [48.41 kcal mol^{-1} compared to **Int (A-4)**]**.** Finally, both HBO fragments of **state (A-5)** return to the **Int (A-2)** system to supply and re-start the cycle C. Thus, by circulation of cycle C, a BH$_3$ is consumed and a methane molecule is released. However, most peaks of cycle C are extremely energy-demanding and require much energy.

Cycle AD, reaction pathways, and products

The results of the molecular dynamic simulations and the PES studies by means of DFT calculations indicate that the most important cycle of the whole system is cycle A–D. As shown in Figures 2, 3, **Int (A-1)** could receive a water molecule and form an **Int (A-1)**-H$_2$O) complex. Then, this complex gains energy and forms TS (A-D) *via* the reaction pathway AD, with a relative PES of 14.70 kcal mol^{-1} [compared to the **Int (A-1)**-H$_2$O complex]. This process is being carried out *via* an electron pair attack from the oxygen of water molecules to the boron atom of **Int (A-1)**. The process continues by proton transfer from the H$_2$O$^+$ fragment to the formate part. By following these changes, **state (A-D)** forms *via* quenching **TS (A-D)**. Two species contain a formic acid molecule and a H$_2$BO fragment in **state (A-D)** (−11.92 kcal mol^{-1}). After completion of cycle AD, the H$_2$BO meta-stable species is released from that cycle *via* reaction path AD to supply **TS (B-3)** of cycle AB. Moreover, formic acid is released, which is both kinetically and thermodynamically favorable. It shows that among all reaction valleys and cyclic complexes, the route in which **Int (A-1)** from cycle AB and forms cycle AD to release formic acid is the most favorable one. Also, there are several reports revealing the fast formation of the six-membered metaboric acid from the transformation of boric acid (Grigorovskaya et al., 2009; Balcı et al., 2012; Hoffendahl et al., 2014).

Figure 4 shows the geometrical structures of several detected species which might emerge during the reduction reaction of CO$_2$ by BH$_3$ species. As shown below, the two reactants approach each other in a unique orientation to form the reactant complex (RC). Then, RC receives energy up to about 15.11 kcal mol^{-1} to form **TS (A-1),** which is significantly favorable compared to **TS (B-1)** (67.99 kcal mol^{-1}). During this transformation, B (1)---H (3) bond is breaking [from 1.85 Å in RC to 1.3 Å in **TS (A-1)**], while B (1)---O (5) (1.65 Å) as well as C (4)---H (3) (1.51 Å) bonds are forming. Then, TS (A-1) loses energy (34.4 kcal mol^{-1}) to form **Int (A-1)**. This species gains energy (44.14 kcal mol^{-1}) to form **TS (A-2)** in which the C (4)---O (5) bond length reaches to 1.84 Å to break totally (as well as transferring H (7) from B (1) to C (4)). Following it, **Int (A-2)** forms, which could release an aldehyde or begin a cycle (C). Alternatively, **Int (A-1)** could react with a water molecule and gain energy to reach **TS (A-D)** *via* the reaction pathway (A-D). As shown in Figure 4, O 8) of the water molecule approaches B (1) and forms **TS (A-D)**. In this species, the distance of the O (8)---B 1) forming bond is about 1.54 Å, while the distances of the B (1)---O (5), and the O (8)---H 9) breaking bonds are 1.67 Å, and 1.29 Å, respectively. It shows that the bond distances in the transition state are more likely to product than to intermediate. The PES data given in Figure 3 confirm these results. Also, it should be noted that **TS (AB-3)** could potentially be considered for the (York and Bell, 2019; Herndon and Whiteside, 2021)-proton-sigmatropic shift reaction due to properties which have recently been revealed in Jasiński, (2020). We have used the B3LYP/6311++G (d,p) level of theory for these mechanism studies due to the fact that this basis set has been widely applied for theoretical prediction of the experimentally investigated reaction parameters. The results of our theoretical studies on the reaction parameters had very good agreement with the previous experimental reports (Siadati et al., 2011; Bekhradnia et al., 2014; Siadati, 2016).

Total circulation of the complex of cycles

The results of the relative PES and the molecular dynamic simulations indicate that the least energy pathway for the reaction between borane and CO$_2$ (the green line in Figure 3) is the reactant complex (**RC**) to **TS (A-1)** to **Int (A-1)** to **TS (A-D)** to formic acid with a relative PES of 0.00 kcal mol^{-1}, +15.11 kcal mol^{-1}, -19.37 kcal mol^{-1}, and +14.70 kcal mol^{-1}, respectively. Thus, among all possible species, formic acid emerges finally from the reaction between CO$_2$ and borane, at least in the gas phase.

As shown in Table 1, the negative frequencies of TSs (A-1) and (A-D), are -457.90, and -1262.52 cm^{-1}, respectively. These strong negative frequencies confirm the reliability of the calculations of the TSs. Also, the $\Delta G^{\#}$ (Gibbs free energy difference) and the $\Delta H^{\#}$ (enthalpy difference) for the formation of TS (A-1) and TS (A–D) are 14.79 kcal mol^{-1}, 19.54 kcal mol^{-1}, 17.57 kcal mol^{-1}, and 18.94 kcal mol^{-1}, respectively. These values indicate the relatively low energy barriers and favorability of the formation of the mentioned TSs in view of thermodynamics, leading to the production of formic acid on the one hand, and metaboric acid, on the other hand.

Conclusion

In the present research, we attempted to follow each of the possible pathways for all of the interactions between CO_2 and borane in order to find the fate of the reaction. The results of the PES studies and also those of the molecular dynamic simulations show that the behaviors of borane and CO_2 lead to the emergence of several possible stable and meta-stable species. Some molecular fragments which are linked to each other by energetic routes and make some related cycles.

The result also indicate that the least energy pathway for the reaction between borane and CO_2 is **RC** to **TS (A-1)** to **Int (A-1)** to **TS (A-D)** to formic acid with relative PESs of 0.00 kcal mol^{-1}, +15.11 kcal mol^{-1}, −19.37 kcal mol^{-1}, +14.70 kcal mol^{-1}, and -11.92 kcal mol^{-1}, respectively. Thus, between all possible species which emerge from the abovementioned complex of cycles, formic acid (and further metaboric acid production from the transformation of boric acid) is formed eventually, at least in the gaseous atmosphere.

Finally, due to the energy barriers and valleys, reduction of CO_2 by borane molecules is possible and even favorable, at least in gas phase. This suggests that the use of gaseous borane (boiling point = 67°C) for reduction of CO_2 should be taken under further consideration by scientists. Investigating any probable meta-stable species (which might emerge during the designation of the whole complex of the reaction cycles) would be a reliable way for understanding the behavior of molecules in the gas phase.

Thus, the outcome of such a project could be helpful for further research in controlling the amount of atmospheric CO_2.

Data availability statement

The original contributions presented in the study are included in the article/Supplementary Material; further inquiries can be directed to the corresponding author.

Author contributions

All the authors listed have made a substantial, direct, and intellectual contribution to the work and approved it for publication.

Conflict of interest

The authors declare that the research was conducted in the absence of any commercial or financial relationships that could be construed as a potential conflict of interest.

Publisher's note

All claims expressed in this article are solely those of the authors and do not necessarily represent those of their affiliated organizations, or those of the publisher, the editors, and the reviewers. Any product that may be evaluated in this article, or claim that may be made by its manufacturer, is not guaranteed or endorsed by the publisher.

Supplementary material

The Supplementary Material for this article can be found online at: https://www.frontiersin.org/articles/10.3389/fchem. 2022.1003086/full#supplementary-material

References

Herndon, J. M., and Whiteside, M. (2021). Intentional destruction of life on earth. *Adv. Soc. Sci. Res. J.* 8, 295–309. doi:10.14738/assrj.87.10597

Abrantes, I., Ferreira, A. F., Silva, A., and Costa, M. (2021). Sustainable aviation fuels and imminent technologies-CO2 emissions evolution towards 2050. *J. Clean. Prod.* 313, 127937. doi:10.1016/j.jclepro.2021.127937

York, R., and Bell, S. E. (2019). Energy transitions or additions?: Why a transition from fossil fuels requires more than the growth of renewable energy. *Energy Res. Soc. Sci.* 51, 40–43. doi:10.1016/j.erss.2019.01.008

Pandey, J. S., Ouyang, Q., and von Solms, N. (2022). New insights into the dissociation of mixed CH4/CO2 hydrates for CH4 production and CO2 storage. *Chem. Eng. J.* 427, 131915. doi:10.1016/j.cej.2021.131915

Liu, Y., Li, B., Lei, X., Liu, S., Zhu, H., Ding, E., et al. (2022). Novel method for high-performance simultaneous removal of NOx and SO2 by coupling yellow phosphorus emulsion with red mud. *Chem. Eng. J.*, 428. Lausanne, Switzerland : 1996. doi:10.1016/j.cej.2021.131991

Yang, Y., Zhu, H., Xu, X., Bao, L., Wang, Y., Lin, H., et al. (2021). Construction of a novel lanthanum carbonate-grafted ZSM-5 zeolite for effective highly selective phosphate removal from wastewater. *Microporous Mesoporous Mater.* 324, 111289. doi:10.1016/j.micromeso.2021.111289

Keijer, T., Bouwens, T., Hessels, J., and Reek, J. N. (2021). Supramolecular strategies in artificial photosynthesis. *Chem. Sci.* 12, 50–70. doi:10.1039/d0sc03715j

Zhao, K., and Quan, X. (2021). Carbon-based materials for electrochemical reduction of CO2 to C2+ oxygenates: Recent progress and remaining challenges. *ACS Catal.* 11, 2076–2097. doi:10.1021/acscatal.0c04714

Lin, X., Li, Z., Liang, B., Zhai, H., Cai, W., Nan, J., et al. (2019). Accelerated microbial reductive dechlorination of 2, 4, 6-trichlorophenol by weak electrical stimulation. *WATER Res.* 162, 236–245. doi:10.1016/j.watres.2019.06.068

Pramudita, R. A., and Motokura, K. (2021). Heterogeneous organocatalysts for the reduction of carbon dioxide with silanes. *ChemSusChem* 14, 281–292. doi:10.1002/cssc.202002300

Porgar, S., and Rahmanian, N. (2022). Phase equilibrium for hydrate formation in the Methane and Ethane system and effect of inhibitors. *Chem. Rev. Lett.* 5, 2–11.

Santos-Carballal, D., Roldan, A., and de Leeuw, N. H. (2021). CO_2 reduction to acetic acid on the greigite Fe3S4 {111} surface. *Faraday Discuss.* 229, 35–49. doi:10.1039/c9fd00141g

Sharghi, H., Aberi, M., Doroodmand, M. M., and Shiri, P. (2017). Chromium (III)-salen complex nanoparticles on AlPO4: As an efficient heterogeneous and reusable nanocatalyst for mild synthesis of highly functionalized piperidines, 2-arylbenzimidazoles, and 2-arylbenzothiazoles. *J. Iran. Chem. Soc.* 14, 1557–1573. doi:10.1007/s13738-017-1097-x

Kadota, K., Duong, N. T., Nishiyama, Y., Sivaniah, E., and Horike, S. (2019). Synthesis of porous coordination polymers using carbon dioxide as a direct source. *Chem. Commun.* 55, 9283–9286. doi:10.1039/c9cc04771a

Kadota, K., Sivaniah, E., and Horike, S. (2020). Reactivity of borohydride incorporated in coordination polymers toward carbon dioxide. *Chem. Commun.* 56, 5111–5114. doi:10.1039/d0cc01753a

Zhu, W., Zhao, J., Wang, L., Teng, Y. L., and Dong, B. X. (2019). Mechanochemical reactions of alkali borohydride with CO_2 under ambient temperature. *J. Solid State Chem.* 277, 828–832. doi:10.1016/j.jssc.2019.07.037

Fujiwara, K., Yasuda, S., and Mizuta, T. (2014). Reduction of CO_2 to trimethoxyboroxine with BH_3 in THF. *Organometallics* 33, 6692–6695. doi:10.1021/om5008488

Bontemps, S. (2016). Boron-mediated activation of carbon dioxide. *Coord. Chem. Rev.* 308, 117–130. doi:10.1016/j.ccr.2015.06.003

Vessally, E., Siadati, S. A., Hosseinian, A., and Edjlali, L. (2017). Selective sensing of ozone and the chemically active gaseous species of the troposphere by using the C_{20} fullerene and graphene segment. *Talanta* 162, 505–510. doi:10.1016/j.talanta.2016.10.010

Li, H., and Zhao, R. (2022). Dissociation of ammonia borane and its subsequent nucleation on the Ru(0001) surface revealed by density functional theoretical simulations. *Phys. Chem. Chem. Phys.* 24, 12226–12235. doi:10.1039/D1CP05957B

Kadhim, M. M., Mahmood, E. A., Abbasi, V., Poor Heravi, M. R., Habibzadeh, S., Mohammadi-Aghdam, S., et al. (2022). Theoretical investigation of the titanium-nitrogen heterofullerenes evolved from the smallest fullerene. *J. Mol. Graph. Model.* 117, 108269. doi:10.1016/j.jmgm.2022.108269

Kadhim, M. M., Mahmood, E. A., Abbasi, V., Poor Heravi, M. R., Habibzadeh, S., Mohammadi-Aghdam, S., et al. (2022). Investigation of the substituted—Titanium nanocages using computational chemistry. *J. Mol. Graph. Model.*, 108317. doi:10.1016/j.jmgm.2022.108317

Siadati, S. A., Amini-Fazl, M. S., and Babanezhad, E. (2016). The possibility of sensing and inactivating the hazardous air pollutant species via adsorption and their [2+ 3] cycloaddition reactions with C_{20} fullerene, Sens. *Actuators B Chem.* 237, 591–596.

Pakravan, P., and Siadati, S. A. (2017). The possibility of using C20 fullerene and graphene as semiconductor segments for detection, and destruction of cyanogen-chloride chemical agent. *J. Mol. Graph. Model.* 75, 80–84. doi:10.1016/j.jmgm.2016.12.001

Siadati, S. A. (2015). An example of a stepwise mechanism for the catalyst-free 1, 3-dipolar cycloaddition between a nitrile oxide and an electron rich alkene. *Tetrahedron Lett.* 56, 4857–4863. doi:10.1016/j.tetlet.2015.06.048

Siadati, S. A., Vessally, E., Hosseinian, A., and Edjlali, L. (2016). Possibility of sensing, adsorbing, and destructing the Tabun-2D-skeletal (Tabun nerve agent) by

C20 fullerene and its boron and nitrogen doped derivatives. *Syn. Mater.* 220, 606–611. doi:10.1016/j.synthmet.2016.08.003

Vessally, E., and Hosseinian, A., A computational study on the some small graphene-Like nanostructures as the anodes in Na–ion Batteries, *Iran. J. Chem. Chem. Eng.* 40 (2021) 691–703.

Kula, K., Kącka-Zych, A., Łapczuk-Krygier, A., and Jasiński, R. (2021). Analysis of the possibility and molecular mechanism of carbon dioxide consumption in the Diels-Alder processes. *Pure Appl. Chem.* 93 (4), 427–446. doi:10.1515/pac-2020-1009

Mohtat, B., Siadati, S. A., Khalilzadeh, M. A., and Zareyee, D. (2018). The concern of emergence of multi-station reaction pathways that might make stepwise the mechanism of the 1, 3-dipolar cycloadditions of azides and alkynes. *J. Mol. Struct.* 1155, 58–64. doi:10.1016/j.molstruc.2017.10.034

Frisch, M. J., Trucks, G. W., Schlegel, H. B., Scuseria, G. E., Robb, M. A., Cheeseman, J. R., et al. (2003). Pittsburgh, PA: Gaussian, Inc.

Becke, A. D. (1988). Density-functional exchange-energy approximation with correct asymptotic behavior. *Phys. Rev. A* 38, 3098–3100. doi:10.1103/physreva.38.3098

Lee, C., Yang, W., and Parr, R. G. (1988). Development of the Colle-Salvetti correlation-energy formula into a functional of the electron density. *Phys. Rev. B* 37, 785–789. doi:10.1103/physrevb.37.785

Peng, C., Ayala, P. Y., Schlegel, H. B., and Frisch, M. J. (1996). Using redundant internal coordinates to optimize equilibrium geometries and transition states. *J. Comput. Chem.* 17, 49–56. doi:10.1002/(sici)1096-987x(19960115)17:1<49:aid-jcc5>3.0.co;2-0

Reed, A. E., Curtiss, L. A., and Weinhold, F. (1988). Intermolecular interactions from a natural bond orbital, donor-acceptor viewpoint. *Chem. Rev.* 88, 899–926. doi:10.1021/cr00088a005

Keith, T. A. (2010). *AIMAll*, 4. Retrieved from aim. tkgristmill. com.Version 10.07. 01.

Domingo, L. R., Kula, K., Ríos-Gutiérrez, M., and Jasinski, R. (2021). Understanding the participation of fluorinated azomethine ylides in carbenoid-type [3+ 2] cycloaddition reactions with ynal systems: A molecular electron density theory study. *J. Org. Chem.* 86, 12644–12653. doi:10.1021/acs.joc.1c01126

Lawan, N., Tinikul, R., Surawatanawong, P., Mulholland, A. J., and Chaiyen, P. (2022). QM/MM molecular modeling reveals mechanism insights into flavin peroxide formation in bacterial luciferase. *J. Chem. Inf. Model.* 62, 399–411. doi:10.1021/acs.jcim.1c01187

Grigorovskaya, V. A., Shashkin, D. P., and Zapadinskii, B. I. (2009). Low-temperature transformations of orthoboric acid. *Russ. J. Phys. Chem. B* 3 (4), 656–660. doi:10.1134/s199079310904023x

Hoffendahl, C., Duquesne, S., Fontaine, G., and Bourbigot, S. (2014). Decomposition mechanism of melamine borate in pyrolytic and thermo-oxidative conditions. *Thermochim. Acta* 590, 73–83. doi:10.1016/j.tca.2014.06.016

Balcı, S., Sezgi, N. A., and Eren, E. (2012). Boron oxide production kinetics using boric acid as raw material. *Ind. Eng. Chem. Res.* 51 (34), 11091–11096. doi:10.1021/ie300685x

Jasiński, R. (2020). On the question of the molecular mechanism of N-nitropyrazole rearrangement. *Chem. Heterocycl. Compd. (N. Y).* 56 (9), 1210–1212. doi:10.1007/s10593-020-02799-x

Siadati, S. A., Nami, N., and Zardoost, M. R. (2011). A DFT study of solvent effects on the cycloaddition of norbornadiene and 3, 4–dihydroisoquinoline-N-oxide. *Prog. React. Kinet. Mech.* 36 (3), 252–258. doi:10.3184/146867811x13095326582455

Siadati, S. A. (2016). Beyond the alternatives that switch the mechanism of the 1, 3-dipolar cycloadditions from concerted to stepwise or vice versa: A literature review. *Prog. React. Kinet. Mech.* 41 (4), 331–344. doi:10.3184/146867816x14719552202168

Bekhradnia, A. R., Arshadi, S., and Siadati, S. A. (2014). 1, 3-Dipolar cycloaddition between substituted phenyl azide and 2, 3-dihydrofuran. *Chem. Pap.* 68 (2), 283–290. doi:10.2478/s11696-013-0440-7